



Applications of artificial neural network (ANN) method for performance prediction of the effect of a vertical 90° bend on an air–silicone oil flow



P.O. Ayegba^{a,*}, M. Abdulkadir^a, V. Hernandez-Perez^c, I.S. Lowndes^b, B.J. Azzopardi^b

^a Department of Chemical Engineering, Federal University of Technology, Minna, P.M.B. 65 Gidan-Kwano, Minna-Bida Road, Niger State, Nigeria

^b Process and Environmental Engineering Research Division, Faculty of Engineering, University of Nottingham, University Park, Nottingham, NG7 2RD, United Kingdom

^c Department of Mechanical Engineering, National University of Singapore, 21 Lower Kent Ridge Rd, 119077, Singapore

ARTICLE INFO

Article history:

Received 5 December 2016

Revised 12 January 2017

Accepted 2 February 2017

Available online 24 February 2017

Keywords:

90° bend

Air–silicone oil

Void fraction

PDF

ANN

Modeling

ABSTRACT

Knowledge of how the presence of a bend can change the flow patterns of a gas–liquid mixture is important for the design of multiphase flow systems, particularly to prevent burn-out and erosion–corrosion. Burn-out and erosion–corrosion both have serious implications for heat and mass transfer. The objective of this work therefore is to train an artificial neural network (ANN), a powerful interpolation technique, to predict the effect of a vertical 90° bend on an air–silicone oil mixture over a wide range of flow rates. Experimental data for training, validation, testing and final prediction were obtained using advanced instrumentation, wire mesh sensor (WMS) and high speed camera. The performance of the models were evaluated using the mean square error (MSE), average absolute relative error (MAE), Chi square test (χ^2) and cross correlation coefficients (R). The performance discriminator χ^2 for prediction of average void fraction is $2.57e-5$ and that for probability density function (PDF) of void fraction MAE is 0.0028 for best performing models. The well trained ANN is then used to predict the effects of the two input parameters individually. The predicted results show that for the before the bend scenario, the most effective input parameter that reflects a change in flow pattern is the gas superficial velocity. On the other hand, the most unfavorable output parameter to measure after the bend is the average void fraction based on the fact that the flow near the bend is a developing one.

© 2017 Taiwan Institute of Chemical Engineers. Published by Elsevier B.V. All rights reserved.

1. Introduction

Pipe fittings such as valves, bends, elbows, tees, reducers, expanders, are integral parts of any piping system. Flow through piping components is more complex than in straight pipes [1]. The presence of a bend can significantly change the flow patterns immediately downstream with the potential of causing damage to the pipe. One common multiphase flow characteristic observed in flows is the redistribution of the flow phases within the bend. This may lead to secondary flows, strongly fluctuating void fractions, flow excursions, flow separations, pressure pulsations and other unsteady flow phenomena [2]. The requirements for economic design, optimization of operating conditions, and evaluation of safety factors create the need for quantitative information about such flows [2].

The possibility of using experimental data to train an Artificial neural network (ANN) in order to predict the redistribution of multiphase flows passing through 90° bends, has received little attention in the peer review literature. Most of the investigations have been restricted to experimental investigation: [2–8] address the issue of gas–liquid systems but most of the reported experiments are not extended to the application of ANN to predict such flows in bends. This paper extends experimental investigation [2] to consider the application of ANN to predict the redistribution of multiphase flows in 90° bends.

Transport processes such as mass, momentum and heat transfer during two-phase gas–liquid flow are vastly influenced by the flow characteristics. For an overall performance and purpose of safety in industrial systems, such as petroleum, biomedical processing systems, chemical and nuclear reactors, it is essential to monitor the flow behavior during normal and transient operations [9]. According to [9], accurate knowledge of flow pattern is necessary in design analysis and rig operation. Probability density function (PDF) of void fraction has been successfully used in the past to characterize flow patterns [8–14]. A number of studies have been carried

* Corresponding author.

E-mail addresses: paulsnow4christ@gmail.com, paulsnow_81@yahoo.com (P.O. Ayegba).

out on the application of ANN for predicting flow characteristics. [15–21] applied ANN for the prediction of hydrodynamic parameters in gas-liquid flow. These studies were limited to flow through straight pipes, however [22] applied ANN for the prediction of frictional pressure drops in U-bends. They claimed that the ANN accurately predicted frictional pressure drop across U-bends.

In general, ANN is widely used in function estimation since it is able to estimate virtually any function in a stable and efficient manner [17]. Therefore, it is expected that the ANN approach can predict the major performance of the effect of bends at arbitrary input conditions without experiment measurements in more industry relevant fluids for the optimal, efficient and safe operation of the flow systems.

2. Material and methods

All experiments were carried out on an inclinable pipe flow rig available within the Engineering Laboratories of the University of Nottingham. Details about the experimental apparatus have been previously reported by [2,23–25]. The experiments were all performed at an ambient laboratory temperature of 20 ± 0.5 °C and a pressure of 1 bar. The behavior of the air–silicone oil mixture was examined using WMS. This technology, described by [26–28], can image the dielectric components in the pipe flow phases by measuring rapidly and continually the capacitances of the passing flow across several crossing points in the mesh.

2.1. Artificial neural network (ANN) modeling

In this work, three different training algorithms from commercial application (MATLAB) were used to configure the network and three different transfer functions (tansig, logsig and purelin) were tested for each training algorithm. The network topography consists of an input layer *IL*, a hidden layer *HL* and an output layer *OL*. The three training algorithms used are; Gradient descent with variable step size and momentum term (GDX); Levenberg Marquardt (LM) algorithm and Resilient back-propagation (RP). Through reliable training and testing using experimental data, the trained ANN can predict the performance of the effect of a bend on air–silicone oil flow. When the ANN is applied to predict the performance of the effect of a bend, it can reveal the highly non-linear relationship between the two input parameters and two output parameters, by searching for optimum weights in its weighting space. Searching for optimal weights or training the ANN aims to minimize a cost function with respect to the training data set. The mathematical background can be found in [12,21,22]. It is worth mentioning that different network topologies are available in ANN but for this work, the back-propagation network with feed-forward algorithm was chosen as this has performed satisfactorily well in previous works [16,18,20,29,30].

3. Results and discussion

3.1. Variation of MSE with number of processing elements in the HL

Table 1 presents the optimum number of processing elements for average void fraction and PDF of void fraction before and after the bend. The number of processing elements which gives the least value of minimum cross-validation MSE is chosen as optimum.

3.1.1. Objective function and performance of ANN

The objective function provides the basis for performance evaluation and network algorithm selection. In this work, sum of squares of error is used as the objective function and is given by

Eq. (1).

$$E = \frac{1}{2} \sum_{i=1}^N (O_i - t_i)^2 \quad (1)$$

Eqs. (2)–(5) are used to check the overall performance of the network. Mean Square Error (MSE), given by;

$$\text{MSE} = \frac{1}{N} \sum_{i=1}^N (O_i - t_i)^2 \quad (2)$$

Mean Absolute Error (MAE), given by;

$$\text{MAE} = \frac{1}{N} \sum_{i=1}^N |O_i - t_i| \quad (3)$$

Chi square test

$$\chi^2 = \sum_{i=1}^N \frac{(O_i - t_i)^2}{t_i} \quad (4)$$

Correlation Coefficient

$$R = \frac{\sum_{i=1}^N (O_i - \bar{O})(t_i - \bar{t})}{\sqrt{\sum_{i=1}^N (O_i - \bar{O})^2 \sum_{i=1}^N (t_i - \bar{t})^2}} \quad (5)$$

The maximum validation test is chosen as six (6) as this produced good results for the problems tested. Network configuration was based on minimum cross validation MSE. It is worth mentioning that the model with the least value of Chi square (χ^2) is taken as the model with best performance when predicting average void fraction. On the other hand, the prediction of PDF of void fraction model performance is based on the Mean Absolute Error (MAE). Thus, the model with the least value of MAE is chosen as the model with the best performance.

3.2. Performance for test and prediction data sets

In this work, test and prediction data sets are used for testing model performance. However, it is worthy of note that while test data set was part of the original network configuration, the prediction data set was not. Since the prediction data set is not included during network configuration, results obtained from it can be used reliably to validate model results obtained from test data, thus minimising the risk of randomization error. While the test data is used here to choose the best performing model, the prediction data set serves as a check for generalization properties of the model.

It can be observed from Table 2 (test data) that all the ANN models tested for the prediction of average void fraction before the bend performed very well. This is seen in the small values of MAE and closeness to unity of *R*. However, Chi square test confirms that the ANN model based on LM algorithm with logsig transfer function and 8 neurons in the hidden layer performed best for the prediction of average void fraction before the bend. Results of Table 2 (prediction data) are a confirmation that all the models tested performed satisfactorily and that the models have good generalization properties.

Table 3 gives performance results for best ANN models for prediction of PDF of void fraction before the bend. It is observed that the ANN model based on LM algorithm with sigmoid transfer function in the *HL* performed very well as can be seen by the small values of MAE and the closeness of *R* to unity. This is further validated by similar results obtained for prediction data.

Table 1
Optimum number of neurons.

Algorithm	Transfer function	Optimum number of processing elements			
		Average void fraction (ε)		PDF of void fraction	
		Before the bend	After the bend	Before the bend	After the bend
GDX	Tansig	4	8	12	11
	Logsig	9	10	12	11
	Purelin	16	2	18	13
LM	Tansig	17	20	12	11
	Logsig	8	6	12	27
	Purelin	6	2	18	16
RP	Tansig	10	14	12	5
	Logsig	8	3	12	14
	Purelin	3	2	11	16

Table 2
Performance of ANN models for prediction of average void fraction before the bend.

	Algorithm	Transfer function	Measurement type (Test data)				Measurement type (Prediction data)			
			MSE	MAE	R	Chi square	MSE	MAE	R	Chi square
Average void fraction	GDX	Tansig	0.0014	0.1915	0.9864	0.0089	0.0015	0.0527	0.9907	0.0021
		Logsig	0.0034	0.2616	0.9902	0.0181	0.0016	0.0521	0.9714	0.0025
		Purelin	0.0107	0.5894	0.9189	0.1113	0.0078	0.1237	0.9542	0.0125
	LM	Tansig	2.50e-4	0.0414	0.9991	5.36e-4	0.0100	0.1119	0.8060	0.0136
		Logsig	9.82e-6	0.0057	0.9999	2.57e-5	5.56e-4	0.0313	0.9674	8.13e-4
		Purelin	0.0110	0.5970	0.9189	0.1156	0.0076	0.1216	0.9541	0.0122
	RP	Tansig	0.0061	0.4141	0.9479	0.0457	4.50e-4	0.0277	0.9694	6.31e-4
		Logsig	0.0014	0.1602	0.9949	0.0067	0.0025	0.0610	0.9410	0.0038
		Purelin	0.0114	0.6143	0.9148	0.1113	0.0130	0.1675	0.9465	0.0204

Table 3
Performance of best ANN models for prediction of PDF of void fraction before the bend.

Algorithm	Transfer function	Measurement type (Test data)			Measurement type (Prediction data)		
		MSE	MAE	R	MSE	MAE	R
GDX	Tansig	3.5041e-4	0.0106	0.5287	2.3702e-4	0.0113	0.5556
	Logsig	2.7497e-4	0.0094	0.6202	1.4472	0.0091	0.5718
	Purelin	3.3954e-4	0.0098	0.4922	1.6428	0.0096	0.4187
LM	Tansig	5.8107e-5	0.0028	0.9335	8.4041e-6	0.0019	0.9750
	Logsig	7.0600e-5	0.0029	0.9189	1.5103e-5	0.0026	0.9550
	Purelin	3.1843E-4	0.0077	0.5413	1.0143e-4	0.0067	0.6441
RP	Tansig	2.0835e-4	0.0065	0.730	1.9297e-4	0.0063	0.6372
	Logsig	2.6266e-4	0.0072	0.6506	1.0159e-4	0.0052	0.7614
	Purelin	2.9992e-4	0.0074	0.5768	1.1360e-4	0.0075	0.5987

3.2.1. Comparison between experimental and predicted PDF of void fraction before the bend

According to [14], a single peak at low void fraction represents bubbly flow while a single peak at low void fraction accompanied by a broadening tail represents spherical cap bubble. On the other hand a double peak feature with one at low void fraction and the other at high void fraction represents slug flow. However, a single peak at high void fraction with a broadening tail represents churn flow.

Fig. 1 shows the comparison between experimental and predicted PDF of void fraction before the bend at liquid and gas superficial velocities of 0.14 ms^{-1} ($0.05\text{--}2.84$) ms^{-1} , respectively.

From the plot, at liquid and gas superficial velocities of 0.14 ms^{-1} and 0.05 ms^{-1} , respectively, both the experimental and predicted PDF of void fraction presents a single peak at low void fraction with a broadening tail extending to a high value of 0.4. This defines a spherical cap bubble flow as in [14]. The flow pattern has been confirmed by the reconstructed images of gas-liquid flow patterns and images of high speed video as shown in Fig. 1a. Thus the degree of agreement between experimental and predicted ANN is good.

When the gas superficial velocity increases to 0.54 ms^{-1} , the spherical cap bubbles coalesce into bullet-shaped Taylor bubbles

and a slug regime is formed. Both the experiment and ANN model (predicted) gives two main peaks at the values of 0.20 and 0.70, respectively. These peaks are the signature of the aerated liquid slugs and the Taylor bubbles with the different sizes. This is also confirmed by the analysis of the reconstructed images of two-phase flow pattern and video images as depicted in Fig. 1b.

At 2.84 ms^{-1} gas superficial velocity, both the experimental and predicted PDF of void fraction shows a single peak at void fraction of about 0.80 with broadened tails, down to 0.3 and 0.92. This is the typical feature of churn.

It is worth mentioning that during the course of carrying out the experimental campaign, it was observed that, the structure of churn flow becomes unstable with the fluid travelling up and down in an oscillatory fashion but with a net upward flow. The instability can be attributed to the relative parity between gravity and shear force acting in opposing direction to the thin film of liquid of Taylor bubbles. Thus, the question begging for an answer therefore here is can the ANN model successfully mimic churn flow and the transition from slug to churn flow (unstable slug flow) with confidence? This section, aims to provide an answer to this interesting question which has serious implications for heat and mass transfer using the PDF of void fraction presented in Fig. 2.

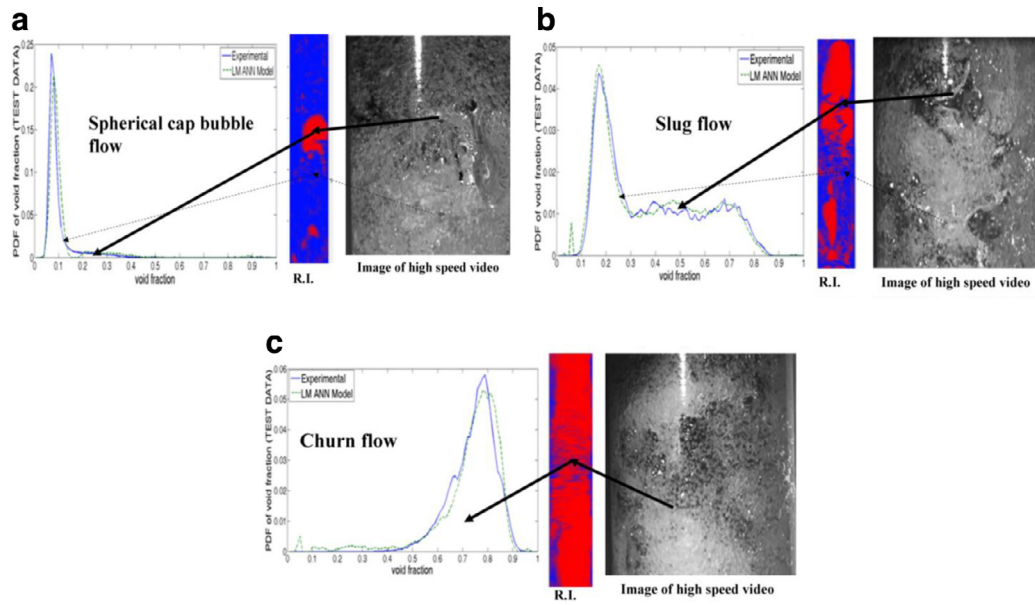


Fig. 1. Experimental and predicted PDF of void fraction before the bend at liquid superficial velocity of 0.14 and gas superficial velocity ($\text{ms}^{-1}0.14$) of: (a) 0.05 (b) 0.54 and (c) 2.84. R.I. represents reconstructed images of two-phase flow pattern. The dash line (a) Represents bubble flow while the thick line spherical cap bubble. On the other hand, the thick line in (b) represents Taylor bubble while the dash line liquid slug. The thick line in (c) represents churn flow.

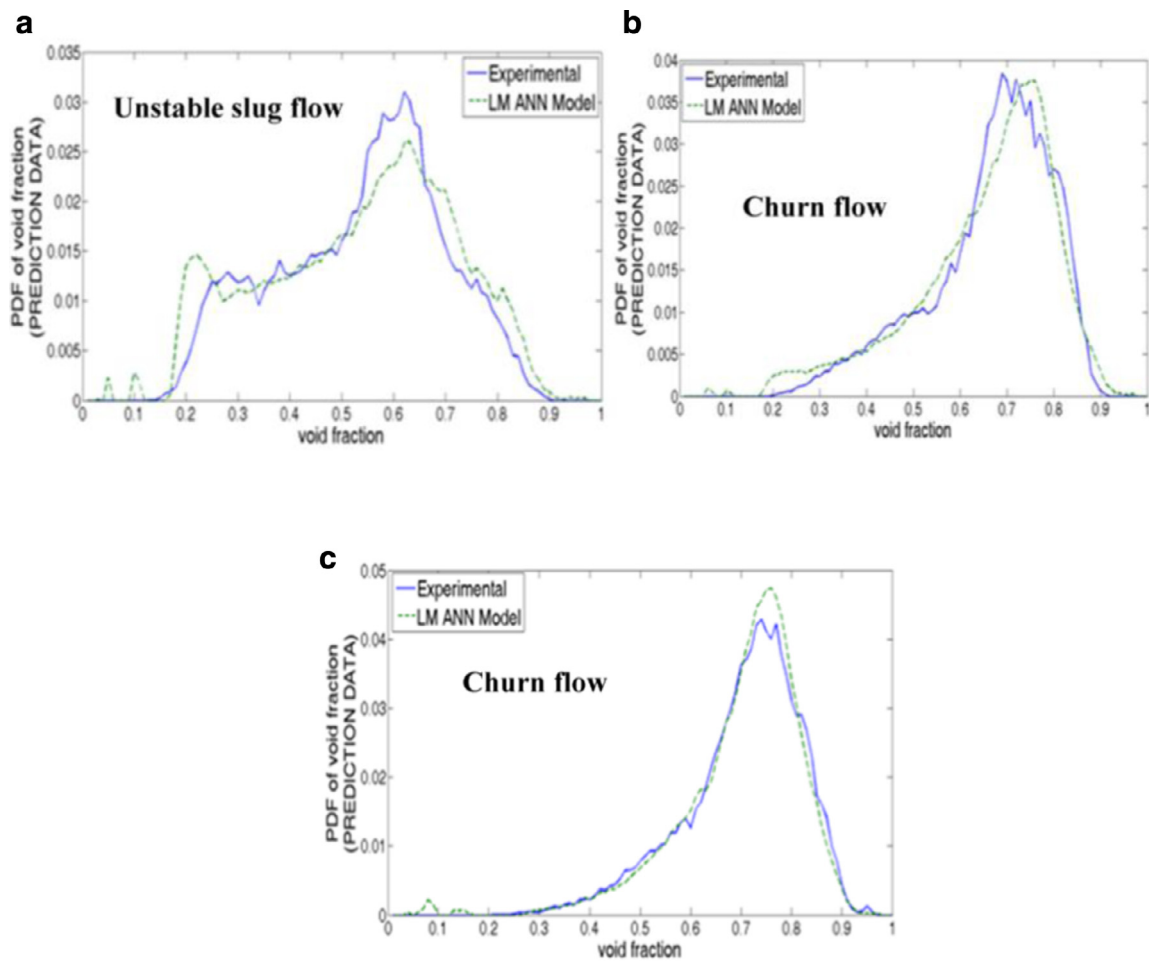


Fig. 2. Experimental and predicted PDF of void fraction at liquid superficial velocity of 0.14 and gas superficial velocity ($\text{ms}^{-1}0.14$) of: (a) 0.95 (b) 1.40 and (c) 1.89.

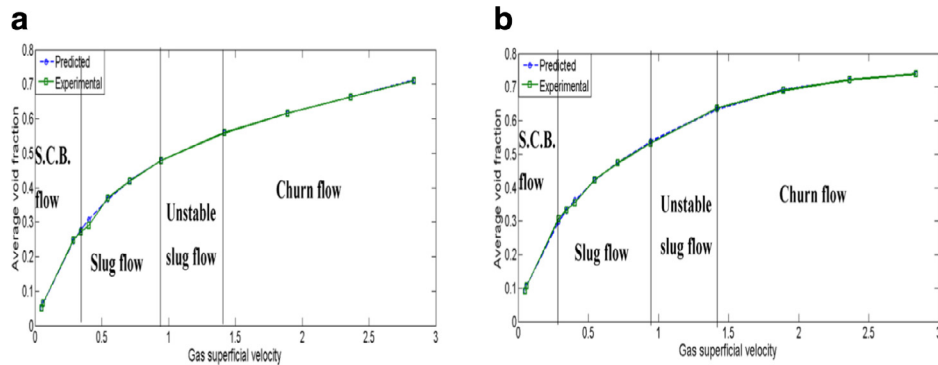


Fig. 3. Comparison of variation of average void fraction with gas superficial velocity obtained from experiments and that predicted using the ANN model based on LM algorithm at liquid superficial velocity ($\text{ms}^{-1}0.14$): (a) 0.14 and (b) 0.38.

Table 4

Summary of comparison between experimental and predicted PDF of void fraction before the bend for both test and prediction data sets.

Flow condition	Test data		Flow condition	Prediction data	
	Experimental	Predicted		Experimental	Predicted
$U_{SL} = 0.05\text{ms}^{-1}0.14$ $U_{SC} = 0.34\text{ms}^{-1}0.14$	Slug flow	Slug flow	$U_{SL} = 0.05\text{ms}^{-1}0.14$ $U_{SC} = 1.42\text{ms}^{-1}0.14$	Churn flow	Churn flow
$U_{SL} = 0.14\text{ms}^{-1}0.14$ $U_{SC} = 0.05\text{ms}^{-1}0.14$	Spherical cap bubble	Spherical cap bubble	$U_{SL} = 0.05\text{ms}^{-1}0.14$ $U_{SC} = 1.89\text{ms}^{-1}0.14$	Churn flow	Churn flow
$U_{SL} = 0.14\text{ms}^{-1}0.14$ $U_{SC} = 0.54\text{ms}^{-1}0.14$	Slug flow	Slug flow	$U_{SL} = 0.05\text{ms}^{-1}0.14$	Churn flow	Churn flow
$U_{SL} = 0.14\text{ms}^{-1}0.14$ $U_{SC} = 2.84\text{ms}^{-1}0.14$	Churn flow	Churn flow	$U_{SL} = 0.14\text{ms}^{-1}0.14$ $U_{SC} = 0.95\text{ms}^{-1}0.14$	Unstable slug flow	Developing slug flow

Table 5

Performance of best ANN models for prediction of average void fraction after the bend.

Algorithm	Transfer function	Measurement type (Test data)				Measurement type (Prediction data)			
		MSE	MAE	R	Chi square	MSE	MAE	R	Chi square
GDX	Tansig	0.0485	0.9778	0.9886	0.2171	0.0106	0.1199	0.9995	0.0123
	Logsig	0.0438	0.9611	0.9993	0.2140	0.0047	0.0659	0.7381	0.0060
	Purelin	0.1055	1.5623	0.8477	0.6016	0.0084	0.0970	0.7477	0.0096
LM	Tansig	0.0346	0.9091	0.9402	0.2647	0.0205	0.1520	0.3408	0.0255
	Logsig	0.1151	1.4591	0.5549	0.5957	0.0147	0.1196	0.3619	0.0166
	Purelin	0.0893	1.3884	0.9047	0.4743	0.0064	0.0736	0.6506	0.0073
RP	Tansig	0.0164	0.2137	0.9972	0.0211	0.0113	0.1001	0.6951	0.0130
	Logsig	0.0841	1.4519	0.9911	0.4972	0.0036	0.0647	0.9901	0.0041
	Purelin	0.1013	1.5486	0.8797	0.5890	0.0042	0.0550	0.6941	0.0047

Interestingly, the ANN model is able to replicate both the unstable slug and churn flows as shown in Fig. 2. At gas superficial velocity of 0.95ms^{-1} , two peaks appear on both the experimental and predicted PDF graph of void fractions. The high value of gas flow rate of 0.95ms^{-1} brings out an increase in Taylor bubbles and the shrinkage of the liquid slugs and as a consequence more and more bubbles are entrained in the liquid slugs. This pattern according to [14] is defined as unstable slug flow.

When the gas superficial velocity reaches 1.40ms^{-1} , the PDF of void fraction for both the experimental and predicted have a single peak with broadened tails down to 0.2 and 0.9. This is the typical feature of churn flow.

At gas superficial velocity of 1.89ms^{-1} , the flow pattern for both the experiment and predicted remain unchanged, churn flow.

Table 4 presents a summary of comparison between experimental and predicted PDF of void fraction before the bend. It can be concluded therefore that the model can be used to predict unstable slug and churn flows before the bend with confidence.

Results of Tables 5 and 6 indicate that all the ANN models tested performed poorly and showed weak generalization properties. This can be attributed to the fact that the flow immediately downstream of the bend is not fully developed. It is interesting, though, to observe from Table 6 that the ANN model based on gradient descent algorithm with logsig transfer function and eleven neurons in the HL performed better than all the other ANN

models tested. It surmises to say that the ANN models cannot be used reliably in the prediction of average void fraction and PDF of void fraction immediately after the bend where the flow is not fully developed.

Tables 5 give performance results of the models tested for the prediction of average void fraction after the bend.

3.2.2. Comparison of experimental and ANN predicted average void fraction over the entire experimental range of gas superficial velocities

An interesting observation made here is that ANN models are able to successfully predict the variation in average void fraction with gas superficial velocity. It can be concluded based on the plots that the best degree of agreement between experiment and predicted average void fraction is observed at liquid superficial velocity of 0.14ms^{-1} , followed by at 0.38ms^{-1} .

Fig. 3 (a) and (b) shows that both the experimental and predicted average void fraction changes with the gas superficial velocity whilst on the other hand decreases with liquid superficial velocity. From the plots, low void fraction values can be observed to be associated with spherical cap bubble and are seen to increase rapidly to slug, unstable slug and churn flows with an increase in gas superficial velocity. This observed trend with regards to average void fraction is consistent with the observations of [31–33].

Table 6
Performance of best ANN models for prediction of PDF of void fraction after the bend.

Algorithm	Transfer function	Measurement type			Measurement type (Prediction data)		
		MSE	MAE	R	MSE	MAE	R
GDX	Tansig	0.0034	0.0195	0.4048	9.3338e-4	0.0155	0.2448
	Logsig	0.0030	0.0186	0.6248	9.5071e-4	0.0149	0.2379
	Purelin	0.0039	0.0209	0.1724	5.2901e-4	0.0167	0.1876
LM	Tansig	0.0048	0.0190	-0.3178	0.0015	0.0109	0.3937
	Logsig	0.0040	0.0211	0.1105	0.0017	0.0145	0.3728
	Purelin	0.0036	0.0189	0.3791	3.6641e-4	0.0099	0.5667
RP	Tansig	0.0039	0.0213	0.1984	2.0884e-4	0.0080	0.7803
	Logsig	0.0038	0.0217	0.2287	7.3632e-4	0.0157	0.2845
	Purelin	0.0037	0.0194	0.3156	3.3291e-4	0.0104	0.5769

4. Conclusion

In this work, the applicability of the use of ANN for estimating the performance of the effect of a vertical 90° bend on an air-silicone oil mixture was demonstrated. A well trained and tested ANN using measurement data is employed to predict its performance at off-design conditions. Especially, the effect of two input parameters (liquid and gas superficial velocities) has been examined. The performance discriminator X^2 for prediction of average void fraction is 2.57e-5 and that for PDF of void fraction MAE is 0.0028 for best performing models. This indicates that there is a good agreement between experimental and ANN predicted results. The predicted results show that the most effective positive influence on the bend is the gas superficial velocity. An increase in gas superficial velocity triggers a change in flow pattern from spherical cap bubble to slug flow then to churn flow and then finally to annular flow. Due to the capability of the neural networks to interpolate, it was applied successfully to predict void fraction outside the range of liquid and gas superficial velocities considered by the experimental work. Therefore, the void fraction and PDF of void fraction including the flow pattern can be predicted with a high degree of accuracy just by knowing the values of liquid and gas superficial velocities using ANNs.

References

- [1] Bandyopadhyay TK, Das SK. Non-Newtonian pseudo-plastic liquid flow through small diameter piping components. *J Pet Sci Eng* 2007;55:156–66.
- [2] Abdulkadir M, et al. Interrogating the effect of 90° bends on air-silicone oil flows using advanced instrumentation. *Chem Eng Sci* 2011;66:2453–67.
- [3] Gardner GC, Neller PH. Phase distributions flow of an air-water mixture round bends and past obstructions. In: *Proceedings of the institution of mechanical engineers*; 1969. p. 93–101.
- [4] Carver MB. Numerical computation of phase separation in two fluid flow. *ASME Pap* 1984;6:153.
- [5] Carver MB, Salcudean M. Three-dimensional numerical modeling of phase distribution of two- fluid flow in elbows and return bends. *Numer Heat Transf* 1986;10:229–51.
- [6] Ellul IR, Issa RI. Prediction of the flow of interspersed gas and liquid phases through pipe bends. *Trans Inst Chem Eng* 1987;65:84–96.
- [7] Legius HJWM, Van-den-Akker HEA. Numerical and experimental analysis of translational gas-liquid pipe flow through a vertical bend. In: *Proceedings of the 8th international conference, BHR group*; 1997.
- [8] Saidj F, et al. Experimental investigation of air-water two-phase flow through vertical 90° bend. *Exp Therm Fluid Sci* 2014;57:226–34.
- [9] Ghosh S, Pratihari DK, Maiti B, Das PK. Identification of flow regimes using conductivity probe signals and neural networks for counter-current gas-liquid two-phase flow. *Chem Eng Sci* 2012;84:417–36.
- [10] Tutu NK. Pressure fluctuations and flow pattern recognition in vertical two-phase gas-liquid flows. *Int J Multiph Flow* 1982;8:443.
- [11] Keska JK, BE W. Experimental comparison of flow pattern detection techniques for air-water mixture flow. *Exp Therm Fluid Sci* 1999;19:1–12.
- [12] Jones OC, Zuber N. The interrelation between void fraction fluctuations and flow pattern in two-phase flow. *Int J Multiph flow* 1975;2:273.
- [13] Vince MA, Lahey RT. On the development of an objective flow regime indicator. *Int J Multiph Flow* 1982;8:93–124.
- [14] Costigan G, Whalley PB. Slug flow regime identification from dynamic void fraction measurements in vertical air-water flows. *Int J Multiph Flow* 1997;23:263–82.
- [15] Nasseh S, Mohebbi A, Jeirani Z, Sarrafi A. Predicting pressure drop in venturi scrubbers with artificial neural networks. *J Hazard Mater* 2007;143:144–9.
- [16] Zhigiang S, Hongjian Z. Neural networks approach for prediction of gas-liquid two-phase flow pattern based on frequency domain analysis of vortex flow meter signals. *Meas Sci Technol* 2008;19:1–8.
- [17] Kumar A, Kumar GK. Artificial neural network based prediction of bed expansion ratio in gas-solid fluidized beds with disk and blade promoters. *Journal* 2004;85:12–16.
- [18] Ayoub MA, Demiral BM. Application of resilient back-propagation neural networks for generating a universal pressure drop model in pipelines. *Univ KHAR-TOUM Eng J* 2011;1:9–21.
- [19] Santoso B, Thomas SW. The identification of gas-liquid co-current two phase flow pattern in a horizontal pipe using the power spectral density and the Artificial neural network (ANN). *Mod Appl Sci* 2012;6:56–67.
- [20] Bar N, Das SK. Gas-non-Newtonian liquid flow through horizontal pipe-gas holdup and pressure drop prediction using multilayer perceptron. *Am J Fluid Dyn* 2012;2:7–16.
- [21] Bar N, Das SK. Prediction of flow regime for air-water flow in circular micro channels using ANN. *J Pet Sci Eng* 2013;10:813–21.
- [22] Bar N, Das SK, Biswas MN. Prediction of frictional pressure drop using Artificial neural network for air-water flow through U-bends. *Procedia Technol* 2013;10:813–21.
- [23] Abdulkadir M, Hernandez-Perez V, Lo S, Lowndes IS, Azzopardi BJ. Comparison of experimental and computational fluid dynamics (CFD) studies of slug flow in a vertical 90° bend. *J Comput Multiph Flows* 2013;5:265–81.
- [24] Abdulkadir M, Hernandez-Perez V, Lowndes IS, Azzopardi BJ. Comparison of experimental and computational fluid dynamics (CFD) studies of slug flow in a vertical riser. *Exp Therm Fluid Sci* 2015;68:468–83.
- [25] Abdulkadir M, Hernandez-Perez V, Lowndes IS, Azzopardi BJ, Brantson ET. Detailed analysis of phase distributions in a vertical riser using wire mesh sensor (WMS). *Exp Therm Fluid Sci* 2014;59:32–42.
- [26] Azzopardi BJ, et al. Wire mesh sensor studies in a vertical pipe. In: *Proceedings of the fifth international conference on multiphase systems*; 2008.
- [27] Manera A, Ozar B, Paranjape S, Ishii M, Prasser H-M. Comparison between wire-mesh-sensors and conducting needle-probes for measurements of two-phase flow parameters. *Nucl Eng Des* 2008;239:1718–24.
- [28] Thiele S, Da-Silva MJ, Hampel U, Abdulkareem L, Azzopardi BJ. High-resolution oil-gas two-phase flow measurement with a new capacitance wire-mesh tomography. In: *Proceedings of the fifth international symposium on process tomography*; 2008. p. 25–6.
- [29] Hao Y, Wilamowski BM. *Industrial electronics handbook: Intelligent systems*. Auburn University; 2010. p. 1–16.
- [30] Mark HB, Martin TH, Howard BD. *Neural network toolbox user's guide R2012b*. The MathWorks Inc; 2012. p. 1–420.
- [31] Omebere-Iyari NK, Azzopardi BJ. A study of flow patterns for gas/liquid flow in small diameter tubes. *Chem Eng Res Des* 2007;85:180–92.
- [32] Bhagwat SM, Ghajar AJ. Similarities and differences in the flow patterns and void fraction in vertical upward and downward two phase flow. *Exp Therm Fluid Sci* 2012;39:213–27.
- [33] Oshinowo T, Charles ME. Vertical two-phase flow- Part 1: flow pattern correlations.. *Can J Chem Eng* 1974;52:25–35.